

# A supervised machine learning estimator for the non-linear matter power spectrum – SEMPS

Irshad Mohammed,<sup>★1,2</sup> and Janu Verma<sup>†3</sup>

<sup>1</sup>*Physik-Institut, University of Zurich, Winterthurerstrasse 190, 8057 Zurich, Switzerland*

<sup>2</sup>*Institute for Computational Science, University of Zurich, Winterthurerstrasse 190, 8057 Zurich, Switzerland*

<sup>3</sup>*Institute for Genomic Diversity, Cornell University, Ithaca 14853, USA*

30 April 2021

## ABSTRACT

In this article, we argue that models based on machine learning (ML) can be very effective in estimating the non-linear matter power spectrum ( $P(k)$ ). We employ the prediction ability of the supervised ML algorithms to build an estimator for the  $P(k)$ . The estimator is trained on a set of cosmological models, and redshifts for which the  $P(k)$  is known, and it learns to predict  $P(k)$  for any other set. We review three ML algorithms — Random Forest, Gradient Boosting Machines, and K-Nearest Neighbours — and investigate their prime parameters to optimize the prediction accuracy of the estimator. We also compute an optimal size of the training set, which is realistic enough, and still yields high accuracy. We find that, employing the optimal values of the internal parameters, a set of 50 – 100 cosmological models is enough to train the estimator that can predict the  $P(k)$  for a wide range of cosmological models, and redshifts. Using this configuration, we build a blackbox — Supervised Estimator for Matter Power Spectrum (SEMPS) — that computes the  $P(k)$  to 5-10% accuracy up to  $k \sim 10h^{-1}\text{Mpc}$  with respect to the reference model (cosmic emulator). We also compare the estimations of SEMPS to that of the Halofit, and find that for the  $k$ -range where the cosmic variance is low, SEMPS estimates are better than that of the Halofit. The predictions of the SEMPS are instantaneous in the sense that it can evaluate up to 500  $P(k)$  in less than one second, which makes it ideal for many applications like visualisations, weak lensing, emulations, likelihood analysis etc.. As a supplement to this article, we provide a publicly available software package<sup>‡</sup>.

## Key words:

(cosmology:) cosmological parameters, cosmology: miscellaneous, (cosmology:) large-scale structure of Universe, methods: numerical, methods: statistical.

## 1 INTRODUCTION

Recently the Planck satellite, employing the cosmological information embedded in the anisotropies of the cosmic microwave background, has put the tightest constraints on the cosmological parameters (Planck Collaboration et al. 2015). This marks the advent of the era of precision cosmology. However, there is a wealth of cosmological information in the large scale structures of the Universe which is not exploited by Planck. The future generation surveys like Euclid (Amendola et al. 2013) and LSST (LSST Science Collaboration et al. 2009) are expected to employ this information to take precision cosmology to the next level.

To achieve this, a thorough understanding of the non-linear structure formation and growth is vital. As the large scale structures of the Universe are the result of gravitational instability of the tiny initial matter density fluctuations, which is a

<sup>‡</sup> <http://www.ics.uzh.ch/~irshad/sempr/>

<sup>★</sup> irshad@physik.uzh.ch

<sup>†</sup> j.verma5@gmail.com

random field, no theory can predict the distribution of matter at any epoch in the cosmic history of time. The best one can hope to achieve is to predict the statistical properties of the density field. The simplest of which is the two-point function or the power spectrum of the density field. In order to employ the constraining power of the future surveys, an accurate modelling of the matter power spectrum is needed up to highly non-linear regime  $k \sim 10 h^{-1}\text{Mpc}$ .

There are various methods to estimate the matter power spectrum which have been successful at various scales. Perturbation theories (for a review see [Durrer \(1994\)](#); [Bernardeau et al. \(2002\)](#)) give the most accurate results, but only up to  $k \sim 0.2 h^{-1}\text{Mpc}$ . The halo model ([McClelland & Silk 1977](#); [Seljak 2000](#); [Cooray & Sheth 2002](#)) framework is computationally faster, but its accuracy is limited only up to  $\sim 30\%$  in the non-linear regime. However, some recent techniques, employing modified version of the halo model, provide very accurate results ([Mohammed & Seljak 2014](#); [Seljak & Vlah 2015](#); [Mead et al. 2015](#)). Halofit ([Smith et al. 2003](#); [Takahashi et al. 2012](#)) provides fitting functions based on cosmological simulations, and the matter power spectrum so evaluated are accurate up to 10% in the non-linear regime. An implementation of the Halofit, called CAMB ([Lewis et al. 2000](#); [Lewis & Challinor 2007](#); [Challinor & Lewis 2011](#)) is widely used. Numerical simulations are the ultimate solution. [Heitmann et al. \(2010\)](#) has developed a cosmic emulator (henceforth Emulator) to evaluate the matter power spectrum based on 38  $N$ -body cosmological simulations. Emulator power spectra are accurate to 3-5 percent up to  $k \sim 10 h^{-1}\text{Mpc}$  on their original cosmological nodes, and lesser so on other sets of cosmological parameters. In addition to the accuracy, the speed of the computation is also an important factor. For example, if the computation of matter power spectrum takes few seconds, the projected weak lensing shear power spectrum will take few minutes, and thus the likelihood analysis of the weak lensing data becomes highly expensive. The developments in this subject in the last few years have been very impressive.

Machine learning has proven to be very effective in solving complex problems in technology (e.g. search, recommendation, spam detection), computational genomic ([Larrañaga et al. \(2006\)](#), [Jensen & Bateman \(2011\)](#)), healthcare ([Pollettini et al. \(2012\)](#), [Chacón & Luci \(2003\)](#)), finance ([Borodin et al. 2011](#)) etc. There has been considerable progress in bridging the gap between machine learning and computational astrophysics, for example the development of the AstroML library ([Vanderplas et al. \(2012\)](#), [Ivezić et al. \(2014\)](#)). In this paper, we employ machine learning based models to estimate the matter power spectrum with great accuracy and speed. We apply the framework of supervised machine learning where a model is trained on a set of cosmological simulations, and it learns to predict the non-linear matter power spectrum over a range of cosmological models, and redshifts with a few percent accuracy. Though the algorithm takes a few seconds to train, the predictions are instantaneous which are ideal for likelihood analyses, e.g., MCMC. We provide a software package (SEMPs) which contains the model trained on a set of cosmologies and redshifts. The power spectrum values can be called from SEMPs for new cosmologies and redshifts. Calls to the trained model retrieve almost instantaneous results for a range of  $k$ -values. The accuracy of such a model will increase as more relevant data (e.g. from independent simulations) is included in the training set.

The advantage over simulations and semi-analytic models is its (i) simplicity, (ii) accuracy which improves with the availability of new data, and (iii) instantaneous speed of predictions.

This paper is organised as follows: We start by introducing the basics of machine learning, and explain the algorithms used in section 2. In section 3, we introduce various datasets, and their configurations important to the analysis. In section 4 we perform an analysis of the intrinsic parameters of the algorithms, and requirements for the data. In section 5, we analyse the performance and accuracy of the predictions for all datasets for their role as training and test set. In section 6, we introduce SEMPs, its main features, accuracy, and efficiency. Finally in section 7, we summarise the article, discuss some important aspects, and finish with some future prospects.

## 2 MACHINE LEARNING

### 2.1 Introduction

Machine learning refers to any systematic way of finding patterns in data, usually for the purpose of making predictions. It works by developing algorithmic models which can be programmed into computers to automatically learn the irregularities in data, and make predictions. The learning algorithm gives computers the ability to learn without being explicitly programmed. The hope is that, with suitable theoretical machinery, we can program computers to emulate the learning mechanism of the human brain. Needless to say, we are far from this goal. See ([Hua et al. 2009](#)) for a quick introduction to machine learning.

In this article, we will restrict to a special class of learning models which fall under *supervised machine learning* (chapter 1 of [Hastie et al. \(2001\)](#)). In these models, the learning is guided by observations with known outcomes. If we have a quantitative output, that we want to predict based on a set of *features*. We prepare a *training set*, which comprises of features and corresponding output values for a set of data points. We choose a supervised machine learning algorithm, which *trains* on the training set, and builds a predictive model, which in turn can predict the output for new unseen data points.

A data point, with its features, is called a *sample* and the corresponding output value is called *target* in machine learning lingo.

The basic setting for a supervised machine learning model is as follows:

- We have a labelled training set i.e. samples with known values of target.
- We are given an unlabelled testing set i.e., samples for which the target values are unknown.
- Goal is to build a model which trains on the labelled data to predict the target for the unlabelled data.

For an introduction to basics of machine learning, refer to the excellent text by Tom Mitchell ([Mitchell 1997](#)). A more mathematical treatment of the subject can be found in ([Hastie et al. 2001](#)). In this article, we will describe three machine learning algorithms for predicting the matter power spectrum.

## 2.2 Algorithms

For the current study, we employed the following supervised machine learning algorithms which will be explained further.

- Random Forests (RF)
- Gradient Boosting Machines (GBM)
- K-Nearest Neighbours (KNN)

In all that follows, the features are expected to be elements of a vector space of dimension equal to number of features ( $p$ , e.g. a set of cosmological parameters). i.e a sample is a tuple of vectors  $(\mathbf{x}, y)$ , where

$$\mathbf{x} = (x_1, x_2, \dots, x_p) \in \mathbb{R}^p \quad (1)$$

and  $y \in \mathbb{R}$  is the target value.

Before we delve into *ensemble methods* (RF, GBM), we have to understand how *decision tree* works for regression.

### Decision Trees :

Decision trees ([Breiman et al. 1984](#)), ([Quinlan 1993](#)) are binary trees, which are formed by recursively partitioning the feature space into smaller, manageable (homogeneous) chunks. The algorithm works by fitting simple models to these chunks. Thus, the complete model comprises of two parts - recursive partitioning of the feature space to construct a tree, and fitting simpler models to the smaller subspaces created in the first step.

For example, consider the situation with only 2 features i.e.  $\mathbf{x} = (x_1, x_2)$  and the output  $y \in \mathbb{R}$ . Let the data points be

$$\begin{aligned} \mathbf{x} &= (0.2, 1.3), y = 0.4 \\ \mathbf{x} &= (0.4, 1.5), y = 0.5 \\ \mathbf{x} &= (1.2, 2.1), y = 0.9 \\ \mathbf{x} &= (1.1, 2.4), y = 1.0 \end{aligned} \quad (2)$$

This data can be partitioned into two subsets as follows :

$$H_1 = (x_1 < 1, x_2 < 2) \text{ and } H_2 = (x_1 > 1, x_2 > 2) \quad (3)$$

Note that this is one of the possible trees, the power of algorithm comes from the fact that it picks best possible tree, in the sense which will be made clear soon.

The algorithm automatically decides the variables to split, value of the variable where split occurs, and the topology of the tree. How does it do that ?

The tree building proceeds with a greedy algorithm. Let  $x_i$  be the splitting variable, with split point  $x_i = l$ , then we get a partition of the feature space as -

$$H_1 = \{\mathbf{x} | x_i < l\} \text{ and } H_2 = \{\mathbf{x} | x_i > l\} \quad (4)$$

And assign target values to each compartment as

$$\hat{y} = \begin{cases} c_1, & \text{for } \mathbf{x} \in H_1 \\ c_2, & \text{for } \mathbf{x} \in H_2 \end{cases} \quad (5)$$

The desired splitting should minimize the total *sum of squares error* in each compartment of the partition of the feature space.

$$S = \sum_{H_i} \sum_{x_j \in H_i} (y_j - c_j)^2 \quad (6)$$

It is not hard to check that the minima occurs at

$$\hat{c}_j = \text{Mean}\{y_j | x_j \in H_i\} \quad (7)$$

This means that each element in the subspace  $H_i \subset \mathbb{R}^p$  is assigned a target value which is equal to the average of the target values in  $H_i$ . This is equivalent to fitting a linear regression in each of the subspaces of the feature space. Notice, we are partitioning, and fitting a simpler model to the training set simultaneously.

In the above example (equation 2), this translates to the assignment

$$\hat{y} = \begin{cases} 0.45, & \text{for } x \in H_1 \\ 0.95, & \text{for } x \in H_2 \end{cases} \quad (8)$$

To summarize, the regression-tree algorithm is as follows :

- (i) Start with a single node containing all the points, no partition.
- (ii) Calculate the estimated target value, and sum of squares error,  $S$
- (iii) Search over all binary splits of all variables to find one which minimizes  $S$ .
- (iv) In each new node, repeat from step (i).

These tree-based methods are very simple conceptually, and are easy to program, yet very potent. We used two such methods in this work, which are described in subsequent sections.

More details on decision trees can be found on chapter 3 of (Mitchell 1997).

### 2.2.1 Random Forests (RF)

Random forests (Breiman 2001) is one of the most powerful machine learning algorithms. A random forest is built from an *ensemble* of decision trees. The idea of ensembling methods (chapter 16 of Hastie et al. (2001)) is to build several models independently, and then the output is taken to be the average of the outputs from the models in the ensemble.

In random forests, an ensemble of trees is constructed where each tree is constructed on a random sample drawn from the training set. The sample is drawn with replacement, it is called *bootstrap sampling* (Efron 1979), (Efron & Tibshirani 1993).

The idea behind RF is to generate multiple little trees from random subsets of data. In that way, each of those small trees gives some group of ill-conditioned (biased) estimators (chapter 15 of (Hastie et al. 2001)). Each of them is capturing different regularities, since random subset of the instances are in the interest. At the extreme randomness, it curates nodes from random subset of the features as well. In this way feature based randomness is also used. After you simply create  $m$  number of trees in this random way, we are able to obtain more cluttered decision boundaries than the simple lines. See chapter 15 of (Hastie et al. 2001) for more details.

### 2.2.2 Gradient Boosting Machines (GBM)

Gradient boosting machines (Friedman 2001), (Friedman 2002) are a class of very effective machine learning algorithms that have shown considerable success in a wide variety of applications. These methods are based on the concept of *boosting* (Breiman 1996), (Freund & Schapire 1997), which means a way to convert *weak learners* to *strong* ones. It provides an answer to the question (Kearns & Valiant 1989) :

*Can a set of weak learning algorithms build a strong one ?.*

Let our training set be

$$T = \{(\mathbf{x}_1, y_1), (\mathbf{x}_2, y_2), \dots, (\mathbf{x}_p, y_p)\} \quad (9)$$

where each  $\mathbf{x}_i \in \mathbb{R}^N$  and each  $y_i \in \mathbb{R}$ . Both  $\mathbf{x}_i$  and  $y_i$  values are known for the training examples.

The goal of supervised learning is to approximate a *decision function*  $F(\mathbf{x})$ , and the estimated value  $\hat{y} = F(\mathbf{x})$ , such that an *error function* ( $E(y, F(\mathbf{x}))$ ) is minimized. In case of linear model, the error function is chosen to be the sum of squares error. This is the same error function, we used for decision trees as well (equation 6).

GBM assumes that the decision function is a linear combination of decision functions of a set of weak learning models. i.e.

$$F(\mathbf{x}) = \sum_{i=1}^K \gamma_i h_i(\mathbf{x}) \quad (10)$$

where  $h_i$ 's are the decision functions of the weak learners and  $\gamma_i$ 's are the corresponding linear coefficients. In this study, we take the weak learners to be the decision trees. Decision trees are particularly valuable for boosting, as they can handle data of mixed type, and model complex functions. In the following, each  $h_i(\mathbf{x})$  is the output of a decision tree trainer.

If  $E(y, F(\mathbf{x}))$  is the error function, we want to find its minima. The GBM algorithm proceeds via gradient descent iteratively as follows :

- (i) Start with a model where each sample is given a constant target value.

$$F_0(\mathbf{x}) = \arg \min_{\gamma} \left( \sum_{j=1}^N E(y_j, \gamma) \right) \quad (11)$$

Here  $\arg \min_x (f(x))$  refers to the value of the argument ( $x$ ) such that the function ( $f$ ) attains its minimum value. In the above situation, the left side of the equation computes the value of  $\gamma$  for which the sum term is minimized.

- (ii) For  $i = 1$  to  $K$  :

- (a) Compute the *residuals*

$$r_{ij} = \frac{\partial E(y_j, F_{i-1}(\mathbf{x}_j))}{\partial F_{i-1}(\mathbf{x}_j)} \quad (12)$$

- (b) Compute the gradient jump

$$\gamma_i = \arg \min_{\gamma} \left( \sum_{j=1}^N E(y_j, F_{i-1}(\mathbf{x}_j) - \gamma r_{ij}) \right) \quad (13)$$

- (c) Update the decision function

$$F_i(\mathbf{x}) = F_{i-1}(\mathbf{x}) + \gamma_i h_i(\mathbf{x}) \quad (14)$$

- (iii) Compute  $F_K(\mathbf{x})$ .

Since we are taking derivatives of the error function in this procedure, it is evident that this algorithm would work for any differentiable error function. For more details refer to chapter 10 of [Hastie et al. \(2001\)](#)

### 2.2.3 K-Nearest Neighbours (KNN)

K-Nearest neighbours ([Altman 1992](#)) is one of the simplest machine learning algorithms which falls under *instance-based learning* methods (chapter 8 of [Mitchell \(1997\)](#)), which means that the computation is deferred until a test case is supplied. The KNN algorithm works by finding K samples from the training set which are closest to the test sample, and the test sample is assigned the target value which is equal to the mean of the target values in the chosen neighbourhood.

As earlier, the feature space of the samples is a real-vector space, and each feature vector has a corresponding target label. To compute the degree of closeness of samples, some distance metric is employed.

The algorithm can be described schematically as follows : Let our training set be

$$T = \{(\mathbf{x}_1, y_1), (\mathbf{x}_2, y_2), \dots, (\mathbf{x}_N, y_N)\} \quad (15)$$

where each  $\mathbf{x}_i \in \mathbb{R}^p$  and each  $y_i \in \mathbb{R}$ . Both  $\mathbf{x}_i$  and  $y_i$  values are known for the training examples.

Let  $\mathbf{x}'$  be a test instance, whose target value we want to predict.

- (i) For each  $\mathbf{x}_i$  in training set, compute its distance from the test case  $\mathbf{x}'$ .

$$\mathfrak{D} = \{(\mathbf{x}, y, d(\mathbf{x}, \mathbf{x}')) | (\mathbf{x}, y) \in T\} \quad (16)$$

where  $d(\mathbf{x}, \mathbf{x}')$  is the distance between  $\mathbf{x}$  and  $\mathbf{x}'$ .

- (ii) Sort  $\mathfrak{D}$  in increasing values of  $d$ .

- (iii) Find the set of K training objects which are closest to  $(\mathbf{x}')$  i.e.

$$S_K \equiv \text{first K entries of } \mathfrak{D} \quad (17)$$

- (iv) Compute the predicted target value for  $\mathbf{x}$ .

$$\hat{y} = \frac{1}{K} \sum_{i=1}^K y_i \quad (18)$$

There are various choices for distance metric e.g Euclidean, Manhattan, Cosine similarity, Minkowski etc.

Another important parameter of this algorithm is the choice of K, number of neighbours are used to compute the prediction. We will study the importance of K in later sections.

KNN is very fast, its speed is proportional to the number of samples in the training data. Its simplicity and speed makes it an ideal model for comparison.

Dataset	Number of cosmological models	Remarks
E38	38	Emulator
ER50	50	Emulator+Random
ER100	100	Emulator+Random
ER1000	1000	Emulator+Random
R50-1	50	Random
R50-2	50	Random
R100-1	100	Random
R100-2	100	Random
R1000-1	1000	Random
R1000-2	1000	Random
R1000-3	1000	Random
NR100-1	100	Normal
NR100-2	100	Normal
NR100-3	100	Normal

**Table 1.** Listing all datasets.

Parameter	Description	Range for Uniform distribution	Mean and std.dev. for normal distribution
$h$	Hubble constant in units $100 \text{ km s}^{-1} \text{ Mpc}^{-1}$	0.65–0.75	(0.7, 0.007)
$\Omega_m$	Normalised matter density at redshift zero	$0.121 < \Omega_m h^2 < 0.154$	$(0.1375/h^2, 0.001/h^2)$
$\Omega_b$	Normalised baryon density at redshift zero	$0.0219 < \Omega_b h^2 < 0.0231$	$(0.0225/h^2, 0.0001/h^2)$
$\sigma_8$	Normalisation of matter power spectrum	0.75–0.84	(0.8, 0.01)
$n_s$	Spectral index	0.9–1.0	(0.96, 0.01)
$w$	Equation of state of dark-energy	−1.1 – −0.9	(−1.0, 0.03)

**Table 2.** Cosmological parameters.

### 3 DATASETS

We used *cosmic emulator* (Heitmann et al. 2010, 2009; Lawrence et al. 2010; Heitmann et al. 2014) to generate different datasets containing the matter power spectrum for different cosmological models and redshifts. Table 1 shows a list of all datasets, and their particulars. We used total 14 datasets of different sizes and configurations.

Two very important ingredients are the choice of redshift and  $k$  arrays (henceforth  $\mathbf{z}$  and  $\mathbf{k}$  respectively). It is desirable that the algorithm learns from various combinations of cosmological models,  $\mathbf{z}$ , and  $\mathbf{k}$ , therefore it is more useful to have randomised arrays in the training dataset rather than fixed. To randomise  $\mathbf{k}$ , and  $\mathbf{z}$ , we follow these two steps:

- Create an array of size  $N_p$ , let us call it *parent array*,
- draw a random subset of size  $N$  from the parent array, let us call it *data array*.

The parent array for  $k$  is taken to be of size 100, which comprises : (i) 10 entries between 0.001 and 0.025, (ii) 50 entries between 0.025 to 1, and (iii) 40 entries between 1 and 10. In each of these ranges the numbers are equally spaced in  $\log_{10}$ . For each cosmological model in every dataset, a data array of size 50 was randomly sampled from the parent array, and power spectrum was computed using the cosmic emulator. The parent array for redshift is also taken to be of size 100. The entries are numbers, equally spaced between 0 and 4.0. The data array is chosen to be of size 20. Therefore, for each cosmological model in every dataset, power spectrum is evaluated for a total of 1000 values ( $50 k \times 20 z$ ). The full dataset has a structure

$$\text{Dataset} \equiv \{\mathbb{C}, \mathbf{k}, \mathbf{z}\}. \quad (19)$$

where,  $\mathbb{C}$  is a set containing six cosmological parameters

$$\mathbb{C} \equiv \{\Omega_m, \sigma_8, h, n_s, \Omega_b, w\}. \quad (20)$$

Table 2 gives a brief description of each cosmological parameter.

We generated four categories of datasets:

- **E38** category contains 38 cosmological models which are the original nodes of the cosmic emulator.
- **RXXX-Y** category contains XXX sets of random cosmological parameters drawn from a uniform distribution. The range of the uniform distribution is given in the table 1. Y is the unique identifier for each RXXX dataset, e.g. the datasets R50-1

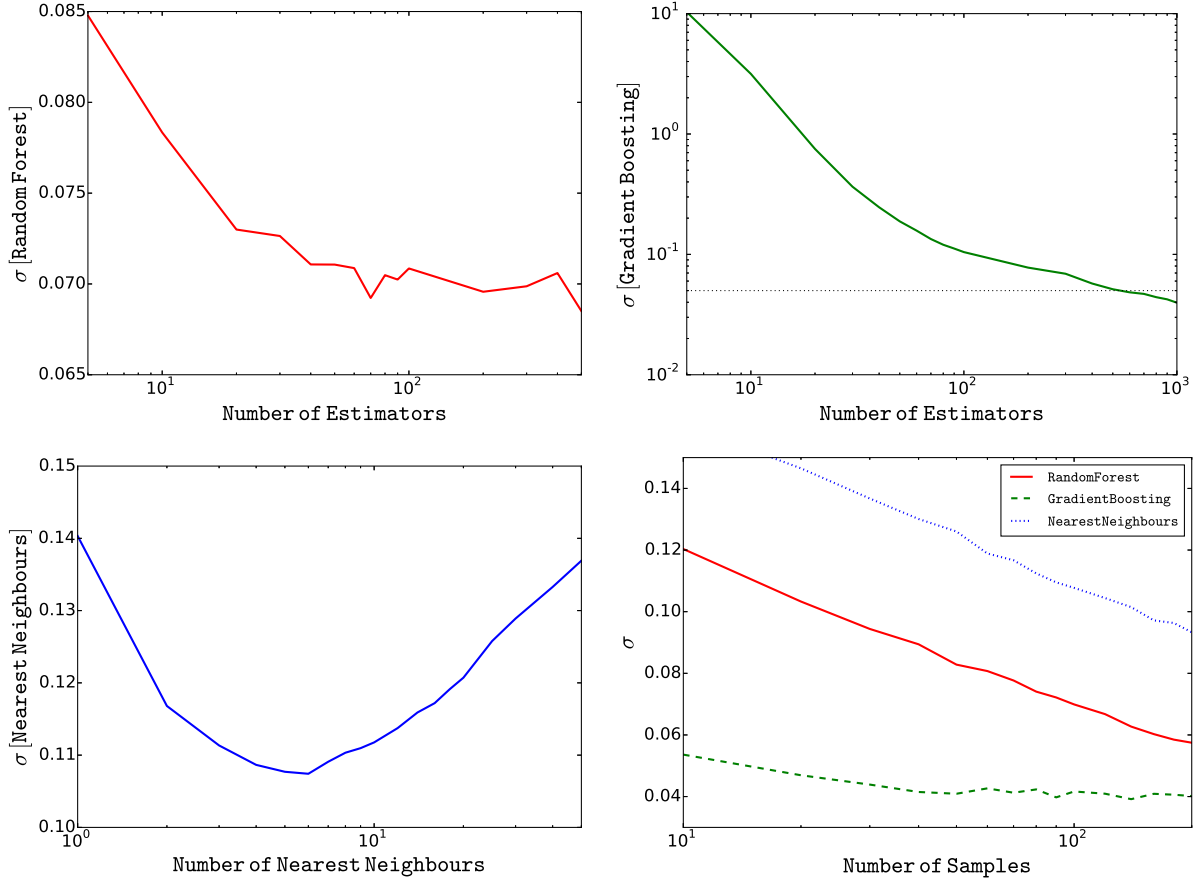


**Figure 1.** First three panels (in reading order) show the variation of the prediction accuracy (in terms of  $\sigma$ ) with the prime internal parameter of each algorithm. Bottom right: Prediction accuracy versus number of samples in the training set for each of the algorithms (parameters set to optimal values)

and R50-2 are two different datasets, each containing 50 sets of random cosmological parameters. 7 such datasets are employed in our study, 2 of size 50, 2 of size 100, and 3 of size 1000.

- **ERXXX** category contains XXX sets of cosmological parameters, 38 of which are the cosmologies from cosmic emulator nodes, the remaining ones are drawn from a uniform distribution of the cosmological parameters (similar to RXXX sets). For example ER100 contains E38 plus R62.

- **NRXXX-Y** category contains XXX sets of cosmological parameters, each of which is drawn from a normal distribution. The mean and standard deviation for each parameter is given in table 1. The unique identifier Y, in this case, resembles the width of the distribution. For example, NR100-2 contains 100 sets of cosmological parameters randomly drawn from a normal distribution with mean and two times the standard deviation width as listed in table 1.

#### 4 PARAMETERS OPTIMIZATION

In this section, we study the parameters of the data mining models to extract their optimal values. We used the **R1000-1** dataset (as described in section 3) for this exercise. This dataset contains 1 million samples, comprising 1000 cosmological models. We used a part of the dataset as the training set, on which we build the models, which we then evaluated on the remaining samples for validation. For each evaluation, we followed these steps :

- Choose an algorithm and fix its parameters.
- Randomly select 10% samples from the R1000-1 as the training set. Assuming perfect randomization, this corresponds to randomly selecting 100 sets of cosmological parameters.
- Train the given algorithm on the chosen training set.
- Predict the power spectra for the remaining 90% samples (test set) based on the trained model.
- Compute the *relative errors* in estimation.



(vi) Compute the *mean* and *standard deviation* for the relative errors.

We did this for a wide range of parameters for each of the three algorithms. At each iteration, a new, random training set is generated. This, hopefully, tames the bias in the estimators, and over-fitting, if any.

A word on notation, let  $(\mathbf{x}, y)$  be a test sample, where  $\mathbf{x}$  is a vector of length 8, containing the cosmological parameters, the redshift value, and the  $k$ -value, and  $y$  is the corresponding value of the power spectrum. We use a model  $M$ , trained on chosen training data, to estimate the value of the power spectrum. Call the estimated value be  $\hat{y}$ . Then the *relative error* is given by the following expression:

$$\delta y_{rel} = \frac{y - \hat{y}}{y} \quad (21)$$

For each test sample, we get a relative error value, and thus, we obtain an array of the size equal to the size of the test set. We compute *mean* ( $\mu$ ) and *standard deviation* ( $\sigma$ ) of this array using the following convention -

$$\mu = \frac{1}{N} \sum_{i=1}^N \delta y_{rel,i}$$

$$\sigma^2 = \frac{1}{N} \sum_{i=1}^N (\delta y_{rel,i} - \mu)^2 \quad (22)$$

where  $\delta y_{rel,i}$  is the relative error of the  $i$ th test example.

We use  $\sigma$  to quantify the prediction accuracy of the algorithm e.g.  $\sigma = 0.05$  implies that 68.3% of the samples are predicted with accuracy better than 5%.

#### 4.1 ML parameters

In this section, we optimize for the prime internal parameter of each algorithm by minimizing  $\sigma$ . As  $\sigma$  quantifies the prediction accuracy, this can be used to identify the best configuration such that the algorithm performs ideally for a realistic choice of the training set.

- **Random Forests:** As we described in the section (3.2), a random forests algorithm is built by taking an ensemble of decision trees. The most important parameter of a random forest based model is the number of trees in the ensemble. We varied the number of trees (herein referred to as *number of estimators*), and recorded the mean and the standard deviation of the relative errors following the aforementioned steps. This is shown in the upper left panel of the figure 1. It can be seen on the picture that the optimal value for number of estimators is near 100.

- **Gradient Boosting:** A gradient boosted tree algorithm, that we used here, is built by fitting an initial set of decision trees on the training set, iteratively modifying the estimates while reducing the error. The parameter of interest in this model is the number of initial decision trees chosen. We fixed all the other internal parameters of the model, and varied the number of trees. The mean and standard deviation of the relative errors of the test set were computed. The variation of the error standard deviation with the variation in the number of decision trees is shown in the upper right panel of the figure 1. The optimal choice for initial trees is around 1000.

- **K-Nearest Neighbours:** The K-Nearest Neighbours algorithm works by estimating the outcome for a test case by averaging the outcomes of its  $K$  neighbours among the training cases. Thus, it is expected that the number of neighbours plays an important role in how accurate the estimation is. We varied the number of neighbours, referred to as  $K$  in our analysis. The bottom left panel of the figure 1 depicts the behaviour of the standard deviation of the relative errors. The graph looks like a parabola, which is very much expected from the description of the algorithm. Initially the number of neighbours is too small to be able to assist in prediction, e.g.  $K = 1$  implies that we base our prediction only on the nearest neighbour. And as we increase the number, we see a drop in the error. This is due to the fact that more neighbours are being used to compute the predicted value. As we keep on increasing  $K$ , after a threshold, a lot of neighbours are creeping into the set we are using for prediction, and a lot of these neighbours are not close enough to have a say in the final prediction. Thus the accuracy drops. We observe the optimal value of  $K$  to be around 5.

#### 4.2 Sample size

We also studied the impact of the size of the training set on the accuracy of the predictions, that we quantified in terms of  $\sigma$  as defined in equation 22. We set the internal parameters of each algorithm to their optimal values as compute in section 4.1.



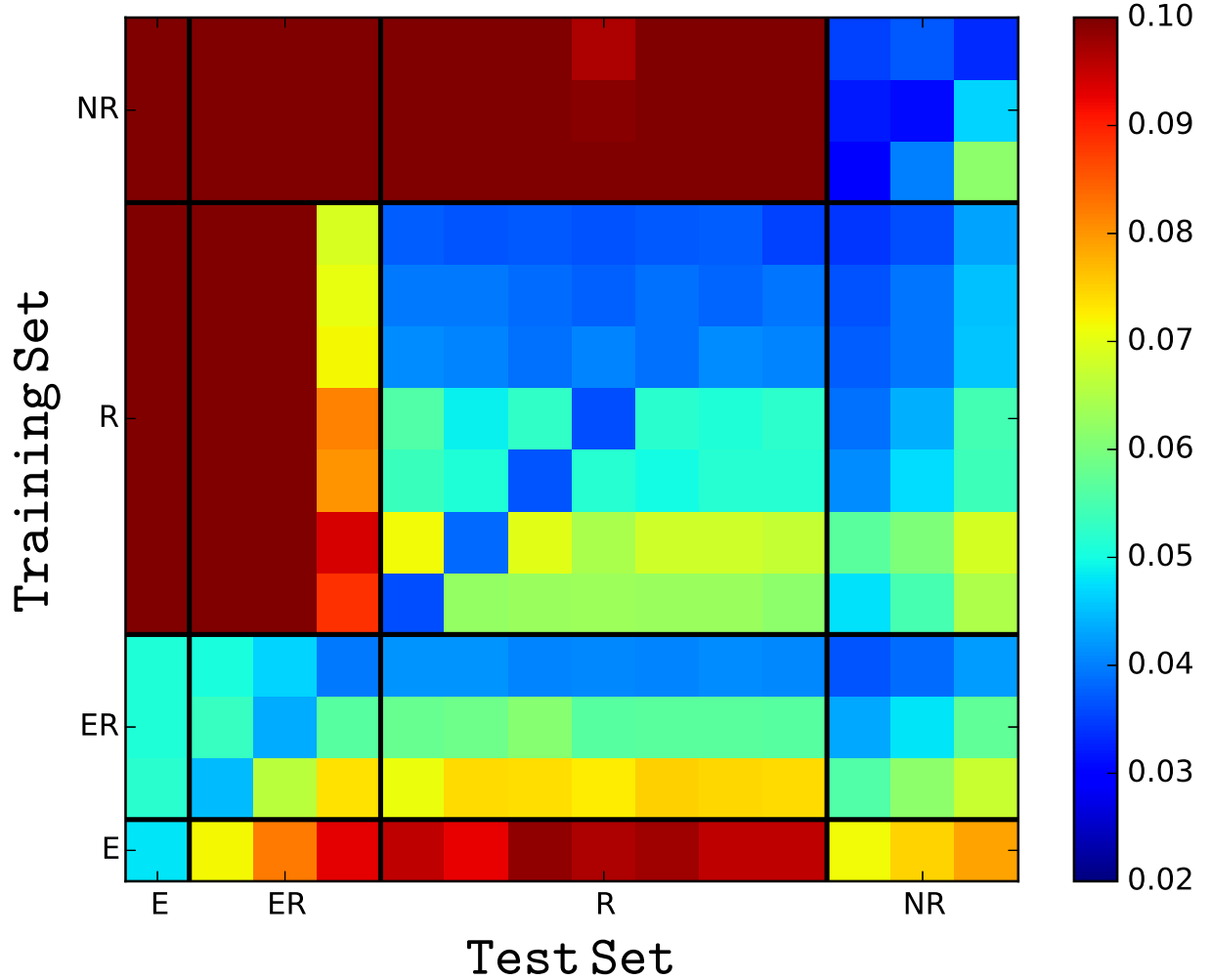


**Figure 2.** Accuracy (in terms of  $\sigma$ ) in color codes for all the permutations of the datasets listed in table 1

Bottom right panel of figure 1 shows the variation of  $\sigma$  with the sample size varying between 10 to 200 cosmological models. As the sample size increases, the predictions in each case become more accurate, which is to be expected.

The gain in accuracy for both KNN and RF is nearly by a factor of two when the size of the training set is increased from 10 to 200, however, RF is performing much better than KNN.

GBM, on the other hand, is doing much better than the other two. With a training set consisting of only 10 sets of cosmological parameters, it can reach to an accuracy corresponding to  $\sigma = 0.06$ . If the size of the training set is increased, there is indeed a slight gain in the accuracy, however  $\sigma$  converges to about 0.04 after the size of the training set exceeds 50 cosmological models. Therefore, if the number of models are limited (which is very much true in actual settings), GBM is the most promising algorithm (of the three we tried) to get sufficiently good predictions over a large range of cosmological models and redshifts.

## 5 PREDICTIONS

We used all datasets listed in table 1, and studied them as both training set and test set for all possible permutations. Figure 2 shows the resulting  $\sigma$  in each case using GBM with 1000 *number of estimators*. Some important features of the analysis are listed below:

- All the training sets can be reproduced (by testing on the training set itself) with an average  $\sigma \sim 0.045$  (the diagonal of the figure 2). It has a small scatter around it, depending upon the **size** of the training set. The best recovered datasets are the ones with size 100, where  $\sigma$  is close to 0.03.

- E38 dataset can reproduce itself with  $\sigma \sim 0.05$ . Testing a trained model on E38 yields a reasonably good accuracy ( $\sigma < 0.1$ ) if the training set contains this set as well. If the E38 set is not included in the training set, we get  $\sigma > 0.1$ .

On the other hand, using only E38 as a training set, cannot predict any other dataset with  $\sigma < 0.07$ .

Thus, to correctly predict the power spectrum of samples in E38, we need to include E38 in the training set, and if only trained on E38, the model crashes for all other test sets.

- ER datasets appear to be the ideal training sets. They can predict E, R as well as NR datasets with  $\sigma < .05$  if the training set comprises of more than 100 training cosmological models. If the size of the ER dataset is larger, the predictions become even better.

- R datasets cannot predict power spectrum for E or ER datasets with good accuracy, however, they predict all random datasets, both R and NR, with  $\sigma \sim 0.04$  for 1000 cosmological models, and slightly larger  $\sigma$  for smaller datasets.

- NR datasets are the worst training sets, except if the test set is also NR. In that case, the prediction is better than any other datasets permutation and reaches  $\sigma \sim 0.03$ .

These observations have solid physical intuition. For example, E38 dataset comprises of the original 38 cosmological nodes of the cosmic emulator, which have more accurate power spectrum compared to the other cosmological models evaluated through interpolation. Therefore, these 38 models have only statistical noise, whereas other models also have a large systematic error. Hence, using E38 as a training set can only predict the power spectrum when the systematic errors are negligible. For all other test cases, like R and NR datasets, this is a highly biased training set.

All R datasets are compatible with each other, and only depend on the sample size for its accuracy of predictions. This is due to the fact that all R datasets comprise of similar systematics, and hence a single learning algorithm can understand all at once.

The NR datasets can be predicted by any training set. This is because the NR datasets have an 6-dimensional Gaussian distribution, and have a very high density near the standard values (listed in table 2). Due to the same reason, NR-1 can be predicted much better than NR-3.

This analysis shows that if E38 models are important, e.g. for a good compatibility with the cosmic emulator, ER datasets make ideal training sets which yield  $\sigma \sim 0.05 - 0.06$  with a realistic number of cosmological models ( $\sim 100$ ). However, if the novelty of E38 data is not a big issue, any random training set containing nearly 100 sets of cosmological parameters yields sufficient good estimates of power spectrum with  $\sigma \sim 0.05$  up to  $k \sim 10 h^{-1} \text{ Mpc}$ .

## 6 SUPERVISED ESTIMATOR FOR MATTER POWER SPECTRUM (SEMPs)

With the collective understanding from previous sections, we build a blackbox called SEMPS — a model trained on ER100 using Gradient Boosting with 1000 number of estimators — and provide it as a supplement to the paper. We performed a few tests to show its productivity and usefulness. Figure 3 shows the cosmological models and the corresponding power spectra of ER100 dataset at redshift zero.

### 6.1 Prediction time

We studied the efficiency of SEMPS on a variable length of  $\mathbf{k}$ . Figure 4 shows the prediction time versus the number of queries made. It is evident that the length of the  $\mathbf{k}$  vector does not matter for the prediction, however, the prediction time goes linearly with number of queries. Therefore, in order to evaluate an observable which is an integrated quantity over the matter power spectrum, for example weak lensing shear power spectrum, 200-500 queries are needed, and hence it can be evaluated in less than one second. To minimize the interpolation errors, power spectrum can be evaluated on a finer  $k$ -array, while the prediction pipeline stays equally efficient.

### 6.2 Comparison with cosmic emulator and CAMB

In this section, we explicitly show the comparison between the matter power spectrum estimation of the SEMPS and the true emulator values. Figure 5 shows the comparison for the E38 dataset (left column), and R100 dataset (right column) at three different redshifts (different rows). In both cases, the predictions are better than 10% accurate up to two sigma, and 5% accurate up to one sigma error bars.

An important aspect is that the predictions of the matter power spectrum in both cases are statistically similar, although both are very distinct datasets. Therefore, SEMPS provides an unbiased estimator. Also, the errors are distributed equally for all  $k$ -ranges, and hence an integrated quantity can average out the noise leaving the observable independent of any systematics.

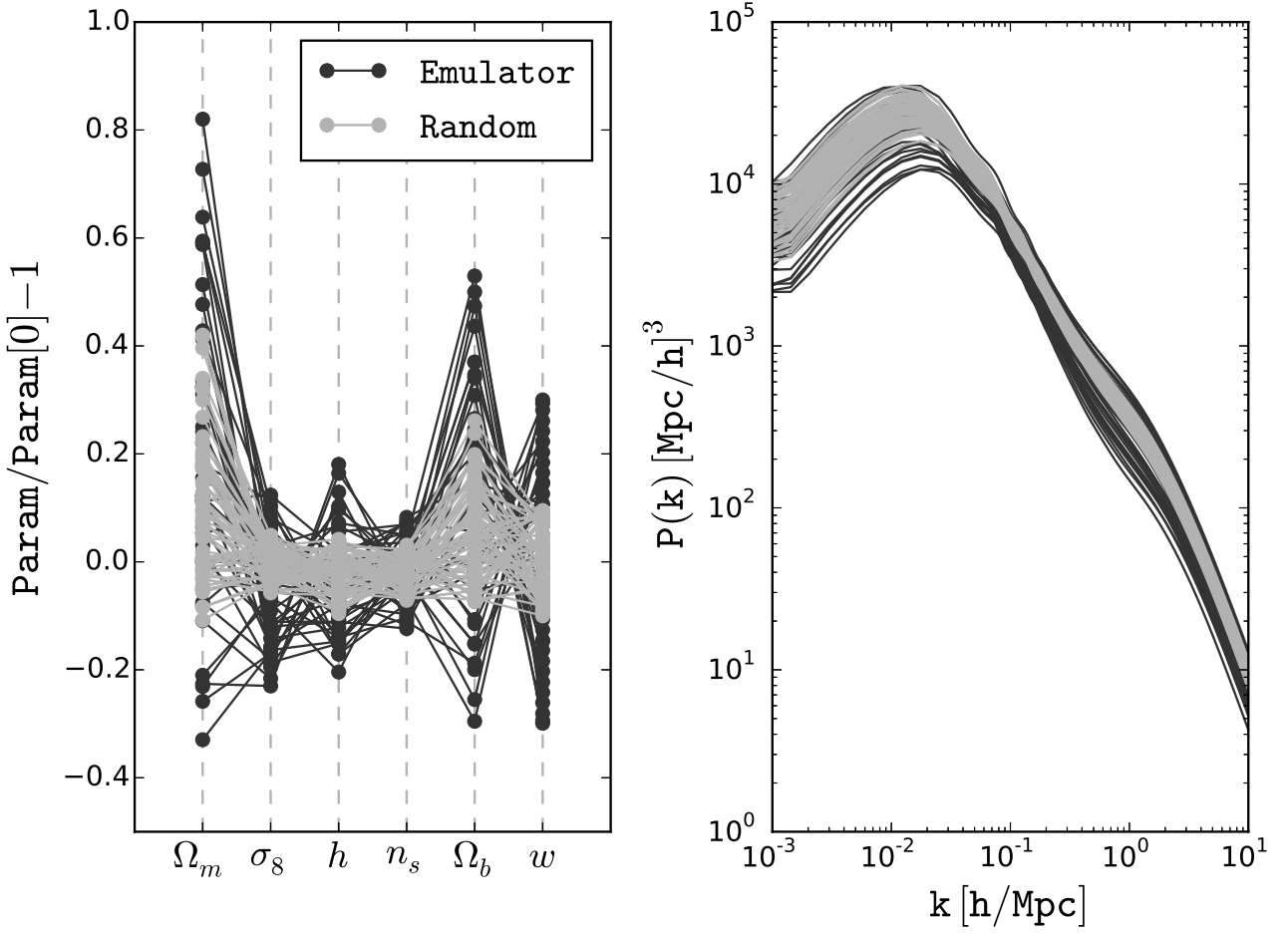


**Figure 3.** Left: 100 cosmological models of ER100 dataset. Right: the corresponding matter power spectra.

In figure 6, we compare the matter power spectrum prediction from both SEMPS and CAMB to the emulator output. For small values of  $k$ , CAMB seems to match better with Emulator compared as to the SEMPS predictions, however, in this regime the cosmic variance is large, and the accuracy is not required. For  $k > 0.1$ , where the cosmic variance drops significantly, SEMPS estimations happen to match better than CAMB predictions.

### 6.3 Software package

An open source python software package for SEMPS is available for use, and further developments. It can be downloaded from <http://www.ics.uzh.ch/~irshad/semps/> as a tar file which contains the code for SEMPS, and an illustrative example file.

## 7 DISCUSSION

In this article, we reviewed three machine learning algorithms — RF, GBM, and KNN — and analysed their usefulness in predicting the matter power spectrum. We also computed the optimal ranges of prime internal parameters for each algorithm which maximize the accuracy for a training set. We found that for RF and GBM, where the parameter under consideration is the number of estimators which controls the complexity of the tree models, it is 100 and 1000 respectively. For KNN, the prime parameter, number of nearest neighbours, has an optimal value of 5. Fixing the optimal values for each prime parameter, we studied the importance of the size of the training set, and found the best behaviour being reported by GBM for all training sets containing 50-100 sets of cosmological parameters (see figure 1).

Inspired by our analysis, we chose GBM with 1000 estimators as the prime algorithm, and studied many different datasets, of different sizes and nature, for their role as training and test sets. We found that the self-predictability of any set is 3-4

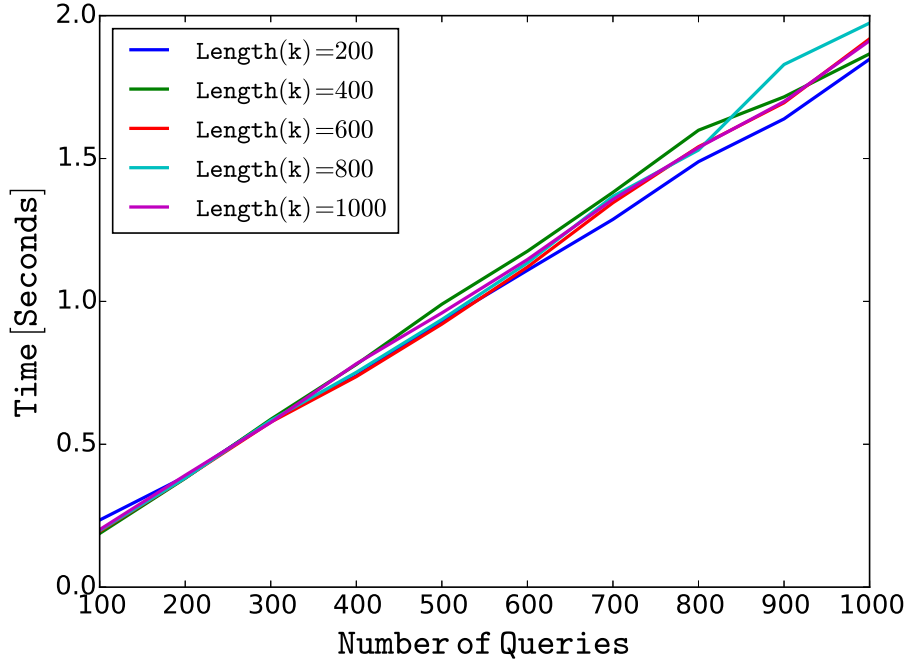


**Figure 4.** Computation time of the matter power spectrum using SEMPS as a function of the number of queries for different lengths of the  $k$ -array.

%, whereas the cross predictability depends on many characteristics (see figure 2). We found that the data generated by the cosmic emulator, E38 dataset, is highly biased in our analysis because it does not share the similar systematics that exist in all other randomly generated datasets, and in order to predict E38 with a good accuracy, those cosmological models have to be included in the training set. However, a random dataset containing 50-100 cosmological models is good enough to estimate a matter power spectrum better than 10% up to  $k \sim 10 h^{-1}$  Mpc for a wide range of cosmological models and redshifts.

We developed an estimator, SEMPS, for the matter power spectrum, which can be used as a blackbox, and is intended to be used this way. It is trained on ER100 (see figure 3) dataset which comprises of a total of 100 cosmological models, 38 of which are cosmic emulator's original nodes, and remaining 62 are random set of cosmological parameters. It was trained using GBM algorithm with a total of 1000 estimators. We analysed the prediction time of the blackbox, and showed explicitly that up to 500 matter power spectra can be computed, for any length of the  $k$ -array, in less than one second (see figure 4). We compared the matter power spectrum predicted from SEMPS to that of the cosmic emulator, and found an agreement of  $\sim 5\%$  up to one-sigma, and  $\sim 10\%$  up to two-sigma for all datasets considered (see figure 5). We also compared the estimations of SEMPS to that of the widely used CAMB, (Halofit). SEMPS is found to be in a better agreement with the emulator values than CAMB (see figure 6).

Our estimations show wiggles for all cosmological models and redshifts. This is due to the reason that it does not have any functional form, but a tree structure that is discrete in nature. On the more optimistic side, these wiggles are distributed uniformly throughout the  $k$ -range, cosmological models and redshifts. Therefore it is possible to average them out by binning in  $k$ , large enough to include the wiggles. Due to the large number of estimators, the scale of these wiggles are very small, and hence a mean matter power spectrum can be derived from SEMPS. However, a major drawback of this method is that it will erase any small scale features, like Baryon Acoustic Oscillations at  $k \sim 0.1 h^{-1}$  Mpc. Therefore, particularly for the applications which do not include BAO feature, this method can supply a smooth matter power spectrum estimator, and not otherwise.

## 7.1 Applications

The accuracy achieved with SEMPS, and its computation being instantaneous, make it an ideal tool for the following cosmological applications.

- **Cosmological observables:** As matter power spectrum underlies many cosmological observables – for example galaxy clustering, weak lensing shear power spectrum etc. – an accurate and unbiased estimation of the matter power spectrum is needed. Particularly, for the weak lensing applications, SEMPS predictions can be very useful as the weak lensing observable

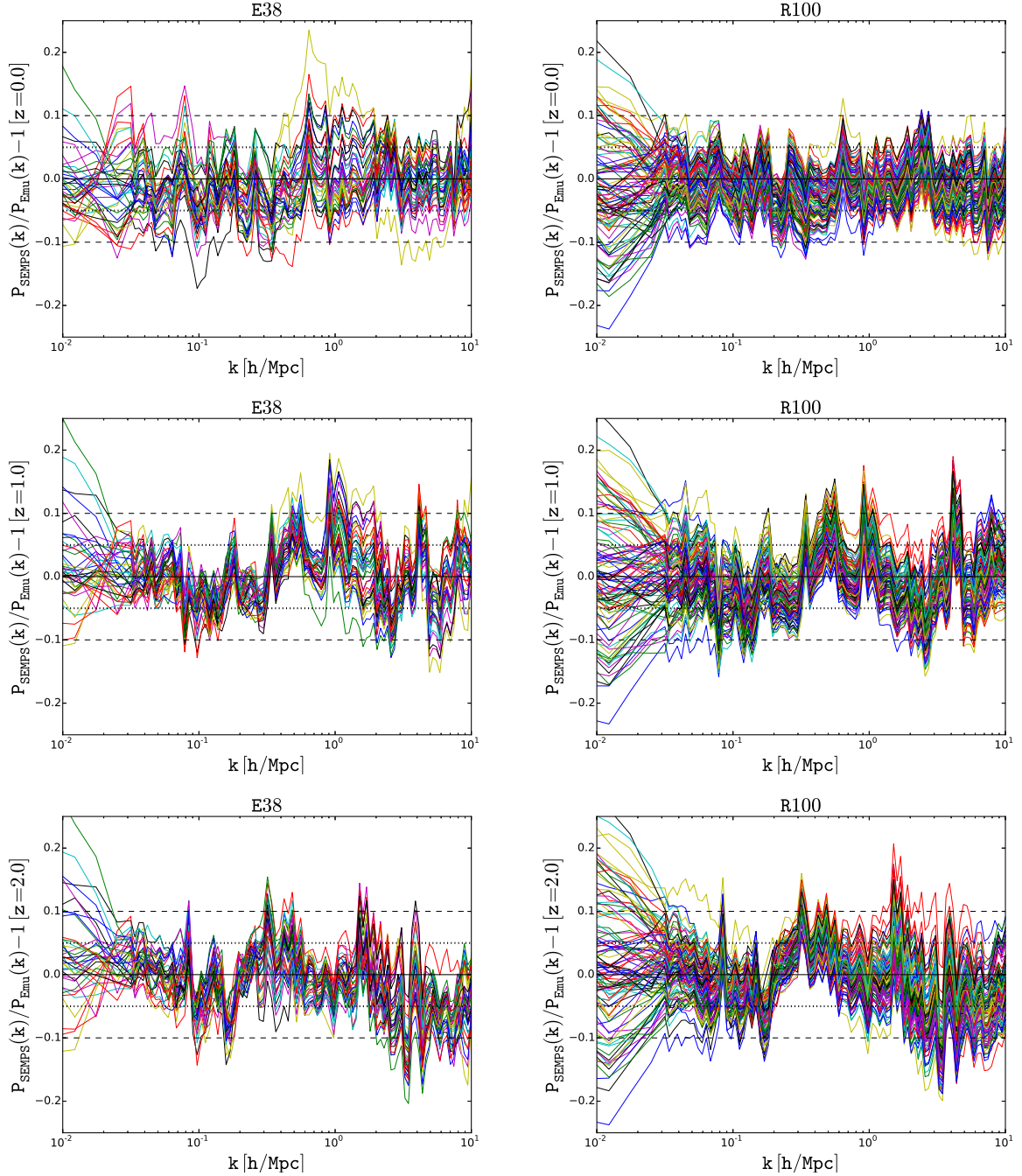


**Figure 5.** Estimates of the matter power spectrum from SEMPS and the emulator for two datasets: E38 (left column) and R100 (right column) for three different redshifts in different rows.

is an integrated quantity of the matter power spectrum over the redshift, it can average out any noise that exist in SEMPS estimates. Also, for this purpose the BAO feature is not very important, so the bin-smoothing of the matter power spectrum can be very useful.

- **Building emulators:** As shown in the analysis that SEMPS predictions are NOT largely biased to its training set, and is predicting the matter power spectrum with noise nearly independent of any cosmological model, it makes it an unbiased estimator. Such estimators can certainly be employed to make emulators for other cosmological observables like galaxy power spectrum, redshift space distortions, two-point correlation function etc.

- **Visualisation:** due to the operational speed of SEMPS, it is possible to build interactive tools to visualise the sensitivity of the matter power spectrum to the cosmological parameters, and redshifts. This can be very useful to explore degeneracies in the cosmological parameters, or simply for educational purposes.



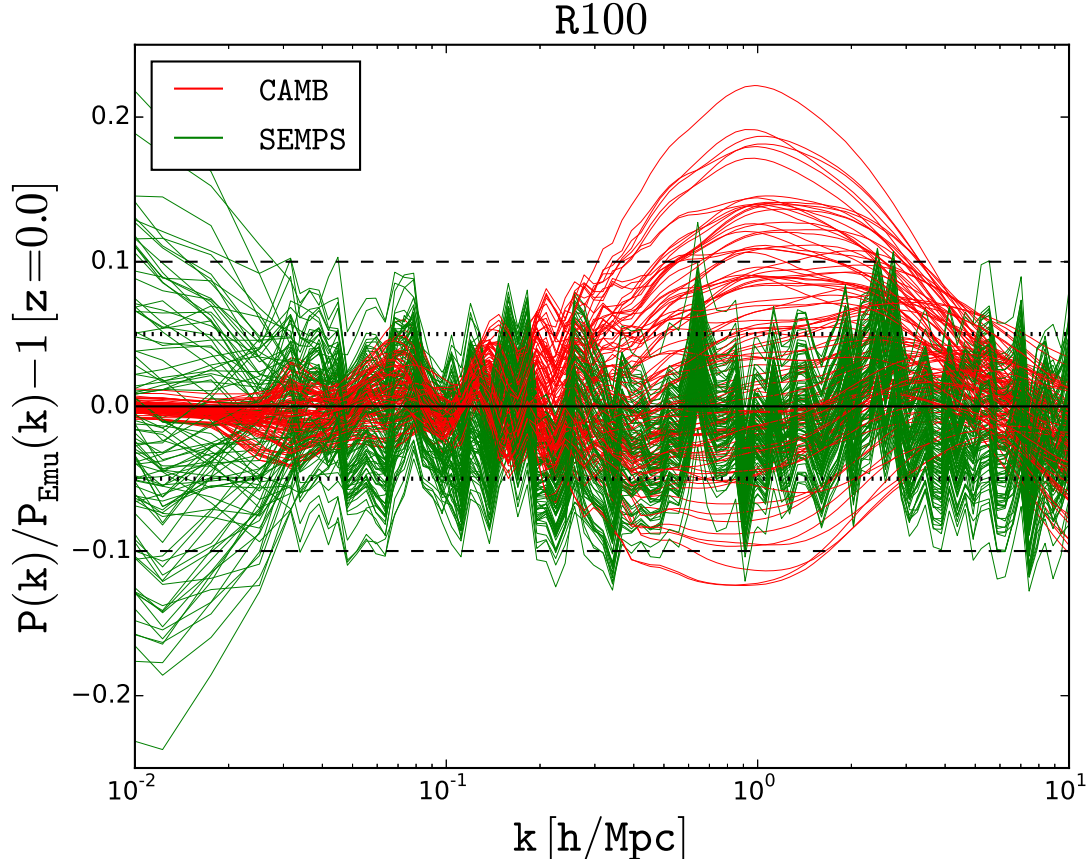


**Figure 6.** Comparison of matter power spectrum estimates from SEMPS and CAMB with those from the emulator on R100 dataset at redshift zero.

## 7.2 Prospects

SEMPS is built on matter power spectra derived from 100 cosmological models computed with the cosmic emulator. The cosmic emulator itself is accurate only up to 5% at its original cosmological nodes, and lesser so for other models. Therefore, the current blackbox is sharing an underlying systematic and interpolation error that were induced by its own training set. To build an improved estimator, a set of 50–100 cosmological simulations can be run, and a similar model can be trained on thus computed matter power spectra. Such an estimator will be independent of any systematic or interpolation errors.

To run such simulations, few million CPU hours would be sufficient. It is certainly possible with the current computational resources that an emulator can easily be built which is light-weight, fast, and accurate. It is also possible to build a flexible emulator system such that new data can be added when available. With current advancements in the computational resources, large cosmological simulations can be run efficiently and inexpensively. In fact, such simulations are being run very often in the cosmological community. Most of these simulations are being run for standard cosmological models derived from recent constraints, for example Planck (Planck Collaboration et al. 2015). Therefore, if power spectra derived from such simulations are added into the training set, the distribution of the cosmological parameters approaches from a uniform to a normal distribution. This will further improve the accuracy of the matter power spectrum estimates in the range overlapping with priors from current data.

## REFERENCES

- Altman N. S., 1992, *The American Statistician*, 46, 175
- Amendola L., et al., 2013, *Living Reviews in Relativity*, 16, 6
- Bernardeau F., Colombi S., Gaztañaga E., Scoccimarro R., 2002, *Physics Reports*, 367, 1
- Borodin A., El-Yaniv R., Gogan V., 2011, preprint, ([arXiv:1107.0036](https://arxiv.org/abs/1107.0036))
- Breiman L., 1996, Technical report, Bias, Variance, and Arcing Classifiers
- Breiman L., 2001, *Mach. Learn.*, 45, 5
- Breiman L., Friedman J. H., Olshen R. A., Stone C. J., 1984, *Classification and Regression Trees*. Wadsworth International Group, Belmont, CA
- Chac  n M., Luci O., 2003, in Sanfeliu A., Ruiz-Shulcloper J., eds, *Lecture Notes in Computer Science*, Vol. 2905, Progress in Pattern Recognition, Speech and Image Analysis. Springer Berlin Heidelberg, pp 350–358, doi:10.1007/978-3-540-24586-5\_43, [http://dx.doi.org/10.1007/978-3-540-24586-5\\_43](http://dx.doi.org/10.1007/978-3-540-24586-5_43)
- Challinor A., Lewis A., 2011, *Phys.Rev.*, D84, 043516
- Cooray A., Sheth R., 2002, *Physics Reports*, 372, 1
- Durrer R., 1994, fcp, 15, 209
- Efron B., 1979, *Ann. Statist.*, 7, 1
- Efron B., Tibshirani R. J., 1993, *An Introduction to the Bootstrap*. Chapman & Hall, New York, NY
- Freund Y., Schapire R. E., 1997, *Journal of Computer and System Sciences*, 55, 119
- Friedman J. H., 2001, *Ann. Statist.*, 29, 1189
- Friedman J. H., 2002, *Comput. Stat. Data Anal.*, 38, 367
- Hastie T., Tibshirani R., Friedman J., 2001, *The Elements of Statistical Learning*. Springer Series in Statistics, Springer New York Inc., New York, NY, USA
- Heitmann K., Higdon D., White M., Habib S., Williams B. J., Lawrence E., Wagner C., 2009, *ApJ*, 705, 156
- Heitmann K., White M., Wagner C., Habib S., Higdon D., 2010, *ApJ*, 715, 104
- Heitmann K., Lawrence E., Kwan J., Habib S., Higdon D., 2014, *ApJ*, 780, 111
- Hua W., Cuiqin M., Lijuan Z., 2009, in *Information Engineering and Computer Science*, 2009. ICIECS 2009. International Conference on. pp 1–4
- Ivezi   Z., Connolly A., Vanderplas J., Gray A., 2014, *Statistics, Data Mining and Machine Learning in Astronomy*. Princeton University Press
- Jensen L. J., Bateman A., 2011, *Bioinformatics*, 27, 3331
- Kearns M., Valiant L. G., 1989, in *Proceedings of the Twenty-first Annual ACM Symposium on Theory of Computing*. STOC ’89. ACM, New York, NY, USA, pp 433–444, doi:10.1145/73007.73049, <http://doi.acm.org/10.1145/73007.73049>
- LSST Science Collaboration et al., 2009, preprint, ([arXiv:0912.0201](https://arxiv.org/abs/0912.0201))
- Larra  saga P., et al., 2006, *Briefings in Bioinformatics*, 7, 86
- Lawrence E., Heitmann K., White M., Higdon D., Wagner C., Habib S., Williams B., 2010, *ApJ*, 713, 1322
- Lewis A., Challinor A., 2007, *Phys.Rev.*, D76, 083005
- Lewis A., Challinor A., Lasenby A., 2000, *Astrophys. J.*, 538, 473
- McClelland J., Silk J., 1977, *ApJ*, 217, 331
- Mead A., Peacock J., Heymans C., Joudaki S., Heavens A., 2015, preprint, ([arXiv:1505.07833](https://arxiv.org/abs/1505.07833))
- Mitchell T. M., 1997, *Machine Learning*, 1 edn. McGraw-Hill, Inc., New York, NY, USA
- Mohammed I., Seljak U., 2014, *MNRAS*, 445, 3382
- Planck Collaboration et al., 2015, preprint, ([arXiv:1502.01589](https://arxiv.org/abs/1502.01589))
- Pollettini J., Panico S., Daneluzzi J., Tin  s R., Baranauskas J., Macedo A., 2012, *Journal of Medical Systems*, 36, 3861
- Quinlan J. R., 1993, *C4.5: Programs for Machine Learning*. Morgan Kaufmann Publishers Inc., San Francisco, CA, USA
- Seljak U., 2000, *MNRAS*, 318, 203
- Seljak U., Vlah Z., 2015, *PRD*, 91, 123516
- Smith R. E., et al., 2003, *Mon. Not. Roy. Astron. Soc.*, 341, 1311
- Takahashi R., Sato M., Nishimichi T., Taruya A., Oguri M., 2012, *ApJ*, 761, 152
- Vanderplas J., Connolly A., Ivezi   Z., Gray A., 2012, in *Conference on Intelligent Data Understanding (CIDU)*. pp 47–54, doi:10.1109/CIDU.2012.6382200